Functional Materials 17, No.3 (2010)

Features of exciton localization in a single *J*-aggregate

I.K.Katrunov, S.L.Yefimova, A.V.Sorokin, Yu.V.Malyukin

Institute for Scintillation Materials, STC "Institute for Single Crystals", National Academy of Sciences of Ukraine, 60 Lenin Ave., 61001 Kharkiv, Ukraine

Received April 2, 2010

Using single molecule spectroscopy technique, exciton localization in a ring *J*-aggregate with average static disorder is $\Delta/\beta \sim 0.3$ has been disclosed. At helium temperature, the *J*-aggregate excitation spectrum consists of a number of resolved spectral lines which are defined by the exponentially localized exciton states ($N_{del} < N_{ring}$) belonging to the nonoverlapping ring segments. The localized exciton spectral properties have been analyzed using a model of strongly curved molecular chain.

С использованием метода одномолекулярной спектроскопии обнаружена локализация экситонов в кольце *J*-агрегата со средней степенью статического беспорядка $\Delta/\beta \sim 0.3$. При гелиевых температурах спектр возбуждения *J*-агрегата состоит из ряда разрешенных спектральных линий, которые определяются экспоненциально локализованными экситонными состояниями ($N_{del} < N_{ring}$), принадлежащими к неперекрывающимся сегментам колец. Спектральные свойства локализованных экситонов проанализированы на основе модели сильно искривленной молекулярной цепочки.

1. Introduction

The long standing interest in the 1D exciton dynamics of systems like conjugated polymers, polysilans and *J*-aggregates is due to their attractive properties in both fundamental and applied sense. *J*-aggregates are nanoscale molecular clusters characterized by a narrow red-shifted exciton absorption band as compared to the monomer one [1–7]. The *J*-aggregate exciton dynamic causes their unique optical properties [1–7] and is resembled to that of the light harvesting complexes [8], thus, *J*-aggregates can be considered as an artificial model thereof [3]. A further *J*-aggregate feature, while remaining in a shadow, could be very attractive for the nanodevice construction: similar to the carbon nanotube electron ballistic transport [9], some types of *J*-aggregates exhibit an anomalous effective exciton migration (~10^6 sites) [6, 10]. From the viewpoint of condensed matter physics, the *J*-aggregates as research objects have stimulated the development of many new ideas and models [1–7, 10].

In the last years, the cryo-TEM technique provides the direct visualization of the *J*-aggregate microscopic structure [4, 11, 12]. The variety of *J*-aggregate architecture depending on properties of building monomers has been revealed [4, 11, 12]. Nevertheless, the molecular chain (linear or ring-shaped) is still the main structure motive of *J*-aggregates. Thus, the concept of 1D Frenkel excitons has been successfully applied to explain the *J*-aggregate optical properties [1–7, 13]. The exciton delocalization length N_{del} defined by the competition between the dipole-dipole interactions and the disorder plays the key role within the frame of 1D exciton model [13–15]. Certainly, the existence of localized exciton states in the disordered systems is connected closely to the Anderson localization phenomenon discussed intensively in [16–18]. The averaged N_{del} can be obtained from a bulk experiment by comparing the absorp-

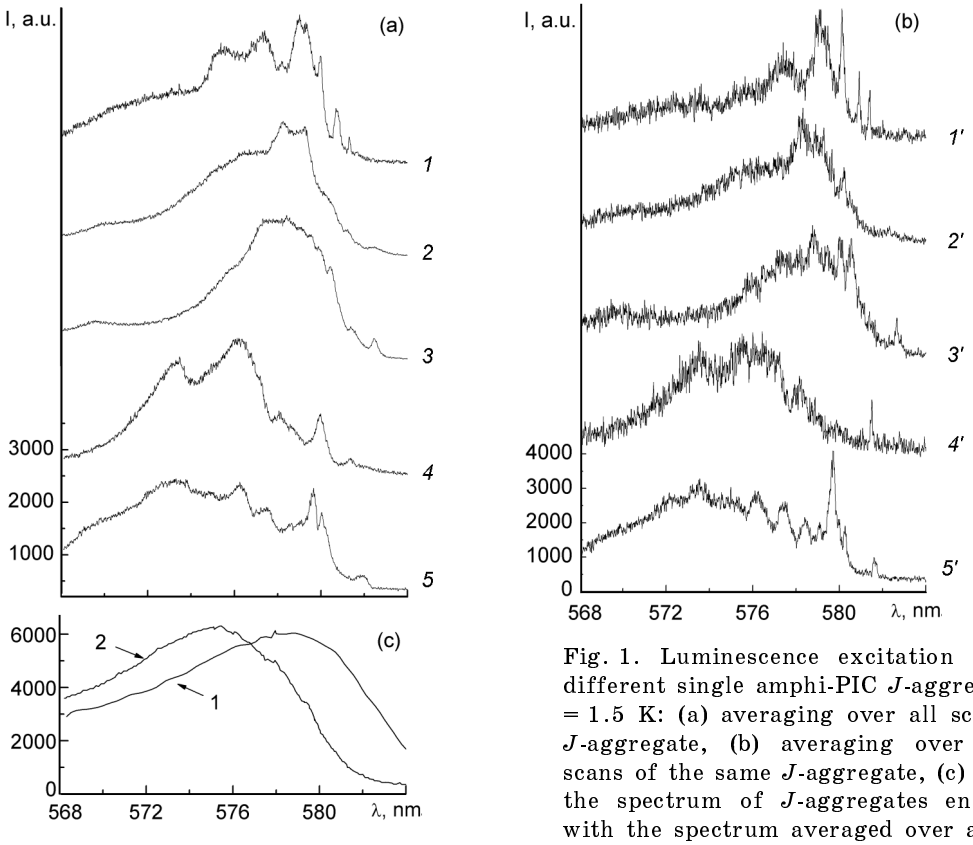

Fig. 1. Luminescence excitation spectra of different single amphi-PIC J-aggregates at T = 1.5 K: (a) averaging over all scans of the J-aggregate, (b) averaging over only few scans of the same J-aggregate, (c) comparing the spectrum of J-aggregates ensemble (*1*) with the spectrum averaged over all individual J-aggregates (*2*).

tion bands or fluorescence decay times of J-aggregates and monomers [1–3, 13], and it is about several tens of monomers (l ~ 100 Å). According to the current concepts, a molecular chain may contain several nonoverlapping segments N_{del} characterized by their intrinsic discrete spectra of local exciton states [13–15], being manifested neither in density of exciton states nor in absorption band [14]. In this connection, the concept of "hidden" structure has appeared [14]. The detailed knowledge about local exciton states will allow looking into microscopic nature of chain excitons and the Anderson localization hypothesis to be examined for 1D exciton system [16–18]. So, it is still an important challenge to find the direct experimental evidence of the existence of discrete spectrum of local exciton states connected with nonoverlapping N_{del} segments.

Room temperatures did not allow to observe quantum effects in spectroscopy of individual J-aggregate of different types [19–22]. Recently, a lot of important experimental results concerning spectroscopy of an individual light harvesting complex have been obtained using the single molecule spectroscopy (SMS) technique [8, 23, 24]. The low-temperature SMS has allowed for the first time to overcome the ensemble averaging and examine the exciton spectra of individual J-aggregates [25]. In the fluorescence excitation spectrum of individual J-aggregate, there were new narrow peculiarities in the low-frequency side as compared to bulk experiments (Fig. 1). These peculiarities have been ascribed to excitons localized on different segments. Unfortunately, the complete picture of exciton localization for single J-aggregates at low temperature is still unclear. The aim of this work is trying to provide a deeper understanding of the results obtained in [25].

2. Experimental section

The study objects were J-aggregates designed from molecules of 1-methyl-1′-octadecyl-2,2′-cyanine perchlorate (amphi-PIC) being an amphiphilic analogue of well-known 1,1′-ethyl-2,2′-cyanine iodide (PIC) molecules (Fig. 2a). The octadecyl radicals allows the amphi-PIC J-aggregates to be formed in a binary dimethylformamide-water (DMF-W) solution at low monomer concentration (~10^{-5} M) [7]. Details of ex-

perimental setup and sample preparation are described in [25].

3. Results and discussion

The W-DMF solutions contained about 90 % of water, thus, under such conditions, the surface-active amphi-PIC molecules can form only a closed structure (Fig. 2). As the dye possesses a large nearly flat "head" resulting in exciton formation due to high translation symmetry, it was supposed that amphi-PIC *J*-aggregates are cylinders consisting of rings including N_{ring} ~ 30 monomers of 3.5 nm diameter dictated by the dye hydrocarbon "tail" [26]. However, cryo-TEM images of amphi-PIC *J*-aggregates revealed large double-wall structures [25]. Here we have to make some remarks to gain a better understanding of the results presented in [25]. At low dye concentrations usually used for amphi-PIC *J*-aggregates preparation, *J*-aggregates are appeared to be too small to obtain their image using cryo-TEM. To resolve the *J*-aggregates, the dye concentration was increased up to 10^{-2} M [25]. For surfactants, it is known that there is a so-called second critical micelle concentration [27]. The increase of the surfactant concentration above the second critical micelle concentration causes the micelle structure transformation from a monolayer to bilayer (lamellar) [27]. Thus, we have supposed that at low dye concentrations, amphi-PIC *J*-aggregates exist in a form of monolayer cylinders of 3.5 nm diameter; a model thereof was proposed in [26]. Similarly, for small TDBC *J*-aggregates unresolvable by cryo-TEM, the single-wall tubular structure also has been proposed [28]. It was stated that small monolayer TDBC *J*-aggregates are formed at low dye concentrations [28], which supports our conclusion about the formation of single-wall amphi-PIC *J*-aggregates at low dye concentrations.

The ensemble of amphi-PIC *J*-aggregates is characterized by a considerable extent of interparticle disorder [29]. It follows from the fact that the summation of several averaged fluorescence excitation spectra of different individual *J*-aggregates does not repeat the bulk fluorescence excitation spectrum (Fig. 1c). The narrow lines vanish as a result of multiple scans summation (Fig. 1c). So, this important observation deserves detailed discussion at a level of single scans.

The fluorescence excitation spectra of individual *J*-aggregates are presented in Fig. 1

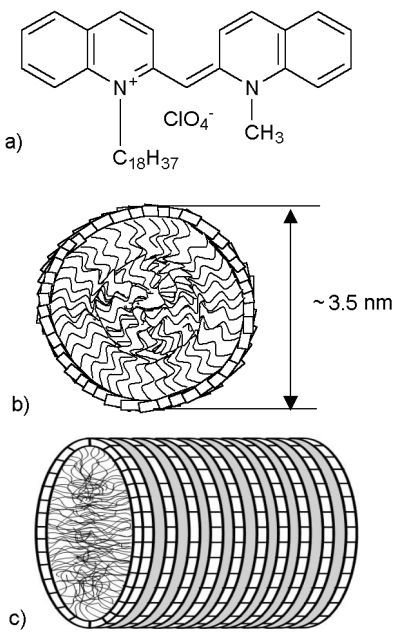

Fig. 2. (a) Molecular structures of amphi-PIC dye, (b) a model of the amphi-PIC ring, (c) a model of cylindrical structure of amphi-PIC *J*-aggregate.

and Fig. 3. The excitation spectra clearly exhibit discrete structure and narrow lines, which have never been observed in bulk spectroscopy neither for amphi-PIC *J*-aggregates nor for others [1–7, 10, 29]. For all individual *J*-aggregates, the excitation spectra exhibit strong fluctuations in the number of spectral lines, their intensity and spectral positions, but the typical structure of spectra is preserved (Fig. 3). It has been revealed that, as a rule, a group of three spectral lines (one narrow long-wavelength line and two broad short-wavelength ones) is observed in each excitation spectrum (Fig. 3, spectrum 1). The narrow line position is fluctuated near 580 nm. Two shifted triplets are often observed in the excitation spectrum (Fig. 3, spectrum 2). The narrow spectral line of the second group is fluctuated around 582 nm. The excitation spectrum containing numerous narrow spectral lines (Fig. 3, spectrum 3) was rarely observed. For some cases, after the certain number of scans (~100), the *J*-aggregate excitation spectrum is not observed at all, while some *J*-aggregates have revealed to be very stable. The narrow lines disappear first, and then the spectrum disappears completely. The remainder of the excitation spectrum after disappearance of the narrow lines is a good evidence that we deal with

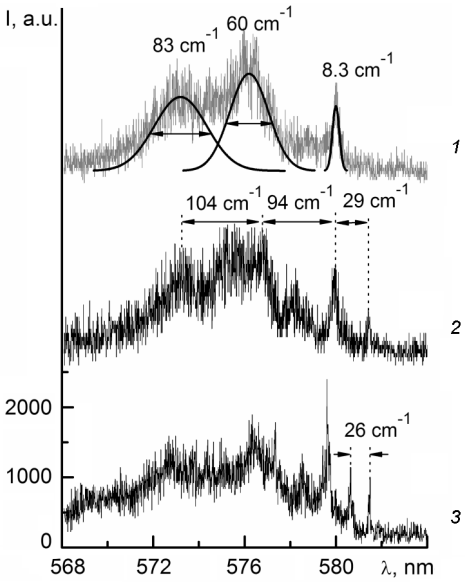

Fig. 3. Characteristic luminescence excitation spectra of single amphi-PIC J-aggregates averaged over only few scans, T = 1.5 K.

photophysical but not photochemical transformations.

Using rotation of laser beam polarization at helium temperatures, it has been established that about 70 % of individual J-aggregates tested do not exhibit any polarization dependence of excitation spectra at all in spite of dipole nature of exciton transition (see Fig. 3 in [25]). However, about 30 % of J-aggregates have shown a prounced polarization dependence (see Fig. 4 in [25]). It can only mean that the exciton transition dipole randomly changes direction in the 360° range. For molecular chain, it could be possible if the chain is long and strongly curved or it is closed.

The strong fluctuation of the excitation spectrum structure with an average splitting less than 100 cm^{-1} and the absence of polarization dependence allow us to suppose that we have found a new type of peculiarities which were hidden by the ensemble averaging in the bulk experiments [7, 29]. It is clear that the logical explanation of the data obtained, in particular, the absence of polarization dependence at low temperatures, will not be achieved within the framework of 1D exciton model used for a ring or linear chain [5, 13]. In an usual treatment, both models predict a pronounced polarization of J-aggregate exciton transitions that has been observed in experiment even at room temperature [19, 28, 30].

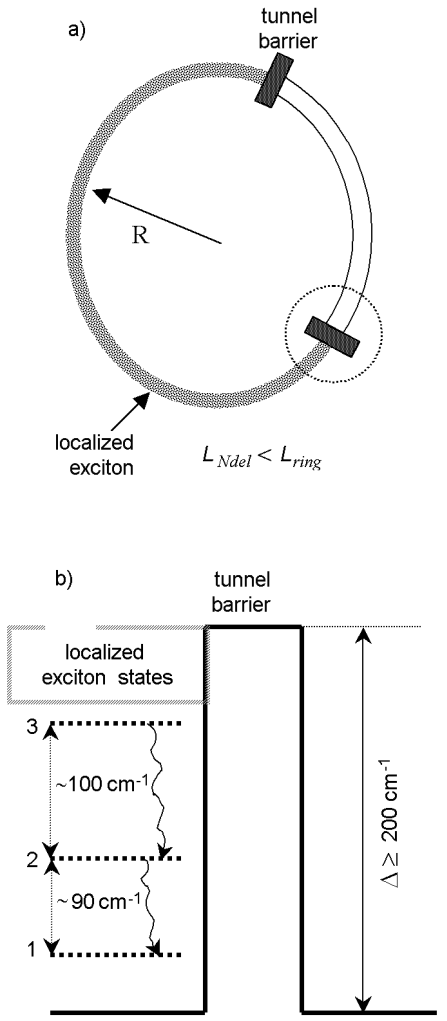

Fig. 4. (a). Simplified scheme of the ring J-aggregate with localized exciton confined by tunnel barriers. The barrier and, respectively, localized exciton positions could be changed under J-aggregate excitation. (b) The simplified scheme of localized exciton states confined by the tunnel barrier, which height is about 200 cm^{-1} or more. The energy parameters characterizing local exciton states are taken from Fig. 3.

Nevertheless, we are going to use both the ring and linear chain models to build an adequate picture of exciton dynamic and temperature transformations observed basing on the analysis of real amphi-PIC J-aggregate structure and nature of the exciton states.

As mentioned above, for the amphi-PIC J-aggregates at helium temperature N_{del} is about 21 monomers. Hence, there could be one N_{del} segment within the ring with discrete spectrum of local exciton states (Fig. 4). This segment is confined by the tunneling barriers which may result from a strong

site energy deviation (Fig. 4). Since at experimental conditions used, only a small number of the rings in the single J-aggregate could be expected, the spectra of excitons localized on different rings are not overlapped. These local exciton states are reflected in the excitation spectrum of individual J-aggregate (Fig. 1 and Fig. 3). The absence of the polarization dependence of J-aggregate excitation spectrum and strong fluctuations of spectral lines predict that positions of the localized exciton within the ring could be changed randomly. So, the exciton transition dipole connected with N_{del} segment takes random orientations on the ring. Of course, under such condition, in spite of the dipole nature of exciton transitions, no polarization dependence of excitation spectra is observed.

In order to get more detailed quantitative information on local exciton states, we start from the chain model of coupled N two-level molecules. We will take into consideration the nearest-neighbor interactions and static diagonal disorder, and neglect phonons. Such type of a quantum system is described by the known exciton Hamiltonian, which can be used for both linear and ring chains [3, 5, 13]:

$$\hat{H} = \sum_n (E_0 + \sigma_n)|n\rangle\langle n| + \sum_n \beta \cdot |n\rangle\langle n+1|. \quad (1)$$

Here, $|n\rangle$ is the state when the molecule n is excited and other molecules are in the ground state; E_0, the site energy; and σ_n, the site energy fluctuation described by the Gauss distribution with $\overline{\sigma_n} = 0$ and $\overline{\sigma_n^2} \neq 0$; β is the transfer integral.

At the condition $\sigma_n = 0$, the exciton states of linear and ring chains are described by the wave functions [3, 5, 13]:

$$\Psi_k = \sqrt{2} \cdot (N+1)^{-1/2} \cdot \sum_{n=1}^{N} \sin\left(\frac{\pi k n}{N+1}\right) \cdot |n\rangle, \quad (2)$$

$$\Psi_k = N^{-1/2} \cdot \sum_{n=1}^{N} \exp\left(i\frac{2\pi k n}{N}\right) \cdot |n\rangle \quad (3)$$

and the exciton spectrum is determined by the equations [3, 5, 13]:

$$E_k = E_0 - 2\beta \cdot \cos(\theta). \quad (4)$$

Here, $\theta = \pi k/N + 1, k = 1,2,...N$ for the linear chain and $\theta = 2\pi k/N, k = 0,\pm1,\pm2,...N/2$ for the ring chain.

To analyze the optical properties and energy spectrum of exciton on N_{del} segment, we can use the linear chain model with some essential remarks. Really, it follows from the excitation spectrum structure (Fig. 3) that three local exciton states are optically active. The linear chain model predicts that odd exciton states (Eq. 2) are optically active but only the bottom $k = 1$ one is characterized by 86 % of full oscillator strength [13]. So, in the linear chain spectrum, only one intense line should be observed. This contradiction is explainable. As it was discussed above, the N_{del} segment length is not much less than N_{ring}, so its curvature is significant. Under this condition, the summation of monomer transition dipoles differs considerably from that for a linear chain due to a variable orientation of monomer dipoles along the N_{del} segment. The exciton transition dipole moment of curved N_{del} segment is nonzero for the odd and even exciton wave functions (2). But, for any $k > 3$, the wave functions (2) exhibit strong oscillation, and the dipole moment of exciton transition tends to zero. Only three exciton transitions ($k = 1, 2, 3$) have significant oscillator strength. It is a reason for the group of three spectral lines observed in the excitation spectra (Fig. 3, spectrum 1). The next contradiction is that the energy intervals between these three lines do not coincide with the exciton spectrum predicted by Eq. 4. The value of the expression $(E_2 - E_1)/(E_3 - E_2)$ is about 0.6 irrespective of β and N_{del} parameter values. At the same time, the value $(\nu_2 - \nu_1)/(\nu_3 - \nu_2)$ is about 1.0 that follows from the spectrum represented in Fig. 3. It follows from experiment that the gap between the first and second local exciton states (~90 cm^{-1}) exceeds the value (~56 cm^{-1}) predicted by Eq. 4.

The static disorder perturbation $V = \sum_n \sigma_n \cdot |n\rangle\langle n|$ of exciton states (Eq. 1) could be one of the reasons for this discrepancy. Really, due to condition $\overline{\sigma_n}$, we have to analyze the second order corrections, which are $\varepsilon_k = \sum_n |V_{k,n}|^2/(E_k - E_n)$, where E_k are the unperturbed energy levels (Eq. 4), ε_1 is negative owing to the condition $(E_1 - E_n) < 0$ and ε_2 is positive due to $(E_2 - E_1) > 0$ and $|(E_2 - E_1)/(E_2 - E_n)| < 1$. Following the same logic, it is possible to show that ε_3 is positive, too. The condition $|\varepsilon_1| > |\varepsilon_2| > |\varepsilon_3| > ... > |\varepsilon_n|$ dictates a remarkable contribution

from corrections to the first energy interval ($k = 1$ and $k = 2$ exciton states). It is important that only two lower exciton states are moved apart and it can be shown that the new value of expression $(E_2 - E_1)/(E_3 - E_2)$ tends to 1. As a rough approximation, the correction to the energy interval between the first and second exciton states is described by the following expression:

$$\varepsilon \sim \varepsilon_1 = \frac{4\theta \cdot \overline{\sigma_n^2}}{(N+1)^2 \cdot (E_2 - E_1)}. \quad (5)$$

Here, θ is about 1, that follows from the summation of harmonic functions.

Hence, the unperturbed energy interval $|E_2 - E_1|$, being about 56 cm^{-1} according to the equation (4), has to be increased by the correction (5), which is about 27 cm^{-1} at $\beta \sim 830$ cm^{-1}, $N_{del} \sim 21$ and $\overline{\sigma_n^2} = (\Delta\nu_{FWHM})^2 = (380\ cm^{-1})^2$ [7, 23]. The new energy interval of 83 cm^{-1} is in agreement with that observed in the excitation spectrum (Fig. 3). Hence, the local exciton states of the ring are formed under the strong influence of the static disorder. In the absence of dephasing, at 1.5 K, the spectral lines of local manifold (Fig. 3, spectrum 1) are characterized by the lifetime limited width. The width of first narrow line of $\Delta\nu_{FWHM} \sim 8.5$ cm^{-1} coincides with the exciton decay time, which is about $70 \cdot 10^{-12}$ s [7]. The width of other two spectral lines is defined by the time of nonradiative relaxation, which is about $0.5 \cdot 10^{-12}$ s for $k = 2$ state and $0.4 \cdot 10^{-12}$ s for $k = 3$ state.

4. Conclusions

The "hidden" spectral structure of J-aggregate localized exciton states has been revealed using the SMS techniques. At helium temperature, in the ring J-aggregate with a considerable static disorder $\Delta/\beta \sim 0.3$, the strong exciton localization regime has been observed. The static disorder effectively confined the local exciton states by tunneling barriers onto N_{del} segments ($N_{del} \sim 21 < N_{ring} \sim 30$ monomers). Under J-aggregate excitation, the positions of N_{del} segments and their characteristics could be changed. The structure of localized exciton spectra demonstrates clearly that the localized exciton states are strongly perturbed due to static disorder.

References

1. J.Moll, S.Daehne, J.Durrant et al., *J.Chem. Phys.*, **102**, 6362 (1995).
2. U.De Rossi, S.Daehne, U.Gomez et al., *J. Phys.Chem.*, **B 102**, 7640 (1998).
3. C.Spitz, J.Knoester, A.Quart et al., *Chem. Phys.*, **275**, 271 (2002).
4. H.Berlepsch, C.Bottcher, A.Quart et al., *J. Phys.Chem.*, **104**, 5255 (2000).
5. S.S.Lampoura, C.Spitz, S.Daehne et al., *J. Phys.Chem.*, **B 106**, 3103 (2002).
6. I.G.Scheblykin, O.Yu.Slusarenko, L.S.Lepnev et al., *J. Phys.Chem.D,* **B 105**, 4636 (2001).
7. G.S.Katrich, K.Kemnitz K., Yu.V.Malyukin, A.M.Ratner, *J. Luminescence*, **90**, 55 (2000).
8. A.M.van Oijen, M.Ketelaars, J.Kohler et al., *Science*, **285**, 400 (1999).
9. P.L.McEuen, M.Bockrath, D.H.Cobden et al., *Phys.Rev.Lett.*, **83**, 5098 (1999).
10. D.Mobius, *Adv.Mater.*, **7**, 437 (1995).
11. H.Berlepsch, C.Bottcher, L.Dahne, *J.Phys. Chem.*, **104**, 8792 (2000).
12. H.Berlepsch, C.Bottcher, *J.Phys.Chem.*, **106**, 3146 (2002).
13. H.Fidder, J.Knoester, D.Wiersma, *J.Chem. Phys.*, **95**, 7880 (1991).
14. A.V.Malyshev, V.A.Malyshev, *Phys.Rev.*, **63**, 195111 (2001).
15. M.Bednarz, V.A.Malyshev, J.Knoester, *J. Chem.Phys.*, **120**, 3827 (2004).
16. F.A.B.F.de Moura, M.L.Lyra, *Phys.Rev.Lett.*, **82**, 3735 (1998).
17. A.Rodriguez, V.A.Malyshev, G.Siera et al., *Phys.Rev.Lett.*, **90**, 027404-1 (2003).
18. F.Dominguez-Adame, V.A.Malyshev, F.A.B.F.de Moura, M.L.Lyra, *Phys.Rev.Lett.*, **91**, 197402-1 (2003).
19. D.A.Higgins, P.E.Barbara, *J.Phys.Chem.*, **99**, 3 (1995).
20. H.Yao, S.Kitamura, K.Kimura, *Phys.Chem. Chem.Phys.*, **3**, 4560 (2001).
21. Yu.V.Malyukin, A.V.Sorokin, S.L.Efimova et al., *J. Luminescence*, **112**, 429 (2005).
22. A.N.Lebedenko, G.Ya.Guralchuk, A.V.Sorokin et al., *J.Phys.Chem.*, **B 110**, 17772 (2006).
23. Ch.Brunel, Ph.Tamarat, B.Lounis et al., *J.Luminescence*, **87–89**, 105 (2000).
24. C.Hofmann, M.Ketelaars, M.Mitsushita et al., *Phys.Rev.Lett.*, **90**, 013004-1 (2003).
25. E.Lang, A.Sorokin, M.Drechsler et al., *Nano Lett.*, **5**, 2635 (2005).
26. Yu.V.Malyukin, S.L.Efimova, A.V.Sorokin et al, *Functional Materials*, **10**, 715 (2003).
27. D.Myers, Surfactant Science and Technology, 3rd Ed. John Wiley & Sons, Inc., Hoboken, New Jersey (2006).
28. C.Spitz, J.Knoester, A.Ouart, S.Daehne, *Chem.Phys.*, **275**, 271 (2002).
29. Yu.V.Malyukin, O.G.Tovmachenko, G.S.Katrich et al., *Low Temp.Phys.*, **24**, 879 (1998).
30. A.V.Sorokin, I.I.Filimonova, R.S.Grynyov et al., *J.Phys.Chem.*, **C 114**, 1299 (2010).

Особливості локалізації екситонів у поодиноких *J*-агрегатах

І.К.Катрунов, С.Л.Єфімова, О.В.Сорокін, Ю.В.Малюкін

За допомогою техніки одномолекулярної спектроскопії виявлено локалізацію екситонів у кільці *J*-агрегату із середнім ступенем статичного безладу $\Delta/\beta \sim 0.3$. При гелієвих температурах спектр збудження *J*-агрегату складається з ряду розрізнених спектральних ліній, які визначаються експоненційно локалізованими екситонними станами ($N_{del} < N_{ring}$), що належать до сегментів кілець, що не перекриваються. Спектральні властивості локалізованих екситонів проаналізовано на основі моделі значно скривленого молекулярного ланцюжка.